



## Embankment Failure in Residual Soils at Nivsar, Ratnagiri

**Ashish Juneja**, Associate Professor, Department of Civil Engineering, Indian Institute of Technology Bombay, Powai, Mumbai 400076 Maharashtra, India; email: [ajuneja@iitb.ac.in](mailto:ajuneja@iitb.ac.in)

**Deblina Chatterjee**, Former graduate student, Department of Civil Engineering, Indian Institute of Technology Bombay, Powai, Mumbai 400076 Maharashtra, India; email: [chatterjeesmail@gmail.com](mailto:chatterjeesmail@gmail.com)

**Rajendra Kumar**, Chief Engineer, Konkan Railway Corporation Ltd., Belapur Bhavan, Plot No. 6, Sector 11, CBD Belapur, Navi Mumbai 400614 Maharashtra, India; email: [ce@konkanrailway.gov.in](mailto:ce@konkanrailway.gov.in)

**ABSTRACT:** *The Nivsar Yard embankment was constructed by the Konkan Railways in 1994. Near the station building, the 22m high embankment runs parallel to the Kajali River for a stretch of about 100m. This stretch has experienced failure and settlement related problems since the record-breaking July 2005 rainfall. Corrective ground improvement measures were implemented immediately after the monsoon. However, these measures were inadequate because the failure surface reappeared during the following monsoon. The failure surface mirrored the shape and size of the failure observed in 2005. Since then after nearly every monsoon, the embankment has moved despite precautionary measures taken by the railway to arrest the movement. The hydrogeological and geotechnical properties which affect slope stability are first discussed. The stability of the embankment is then evaluated at 5 sections drawn along the slope. Two cases are considered. In the first case, the stability of the unreinforced slope is calculated. In the second case, calculations are done using the slope reinforced with soil nails and micropiles installed in 2005 and 2007. The design railway loading and the water level position during the dry and wet season were also taken into account in the stability analysis. The safety factor during the wet season was observed to be less than unity in 4 out of 5 sections for both cases. In each case, the critical circle passed through the toe of the embankment and mirrored the field observations. In 2010-11, the rail tracks were realigned to bypass the failure surface. The stability of the slope was reinvestigated and considered to be safe under the new loads. Irrespective of the above change in the rail alignment, the cumulative settlement of the embankment has also reduced since the 2009 monsoon.*

**KEYWORDS:** Embankment failure, ground improvement, residual soils, simplified Bishop method, stability number.

**SITE LOCATION:** [IJGCH-database.kmz](#) (requires Google Earth)

### INTRODUCTION

Nivsar is located in Ratnagiri district of Maharashtra at latitude  $16.95^{\circ}$  N and longitude  $73.45^{\circ}$  E. Most of the rain in this region falls during the monsoon which lasts from mid-June to mid-September. Konkan Railways pass through this district and has a station located at Nivsar. Figure 1 shows the location of the station building. A portion of the approach earthfill embankment (shown by broken line in the figure) has experienced failure and settlement related problems since the 2005 monsoon. The failure surface at the embankment follows the shape of an inverted parabola and encompasses all the rail tracks and the station platform. The slip circle appears to pass through the toe of the embankment and terminates close to the road, where transverse cracks are observed.

### BACKGROUND

The Nivsar Yard Embankment was opened to rail traffic in 1997. In that same year, a slope failed in between chainage km 218.1 and 218.2. Because the failure (slip) circle was below the railway foundation level, the entire rail track shifted away and the ground heaved (RDSO, 2005). Other than the above incident, no other embankment failure was documented at the

Submitted: 19 July 2012; Published: 25 April 2013

Reference: Juneja, A., Chatterjee, D., and Kumar, R. (2013). *Embankment Failure in Residual Soils at Nivsar Ratnagiri*. International Journal of Geoengineering Case histories,

<http://casehistories.geoengineer.org>, Vol.2, Issue 3, p.229-251. doi: 10.4417/IJGCH-02-03-04



site until the year 2005. In that year, cracks in the embankment developed between chainage km 218.8 and 218.9 following record-breaking rainfall. Heavy rain occurred for 3 days between July 24<sup>th</sup> and 26<sup>th</sup>. Cracks opened up to 20mm width over a period of 15 to 20 days. During the same time, the slope settled by more than 150mm. The total settlement was about 550mm towards the end of the 2005 monsoon. At the end of this period, the cracks took shape of a parabola with its vertex close to the station platform. The parabola sloped downhill for about 100 to 120m towards the river. Figure 2 shows the extent of the slope failure observed in 2005.

Soon after the observed failure, and when the 2005 monsoon was over, soil nails and micro-piles were installed to prevent further damage to the embankment. Table 1 shows details of the ground improvement works undertaken at the site in 2005. However, the 100mm wide and 130m long crack reappeared during the 2006 monsoon. As in the previous year, the crack encompassed all 3 railway lines, including the main line. The shape and size of the crack mirrored the shape and size observed following the 2005 monsoon. The embankment settled throughout the 2006 monsoon reaching a high value of 2930mm at the station platform.

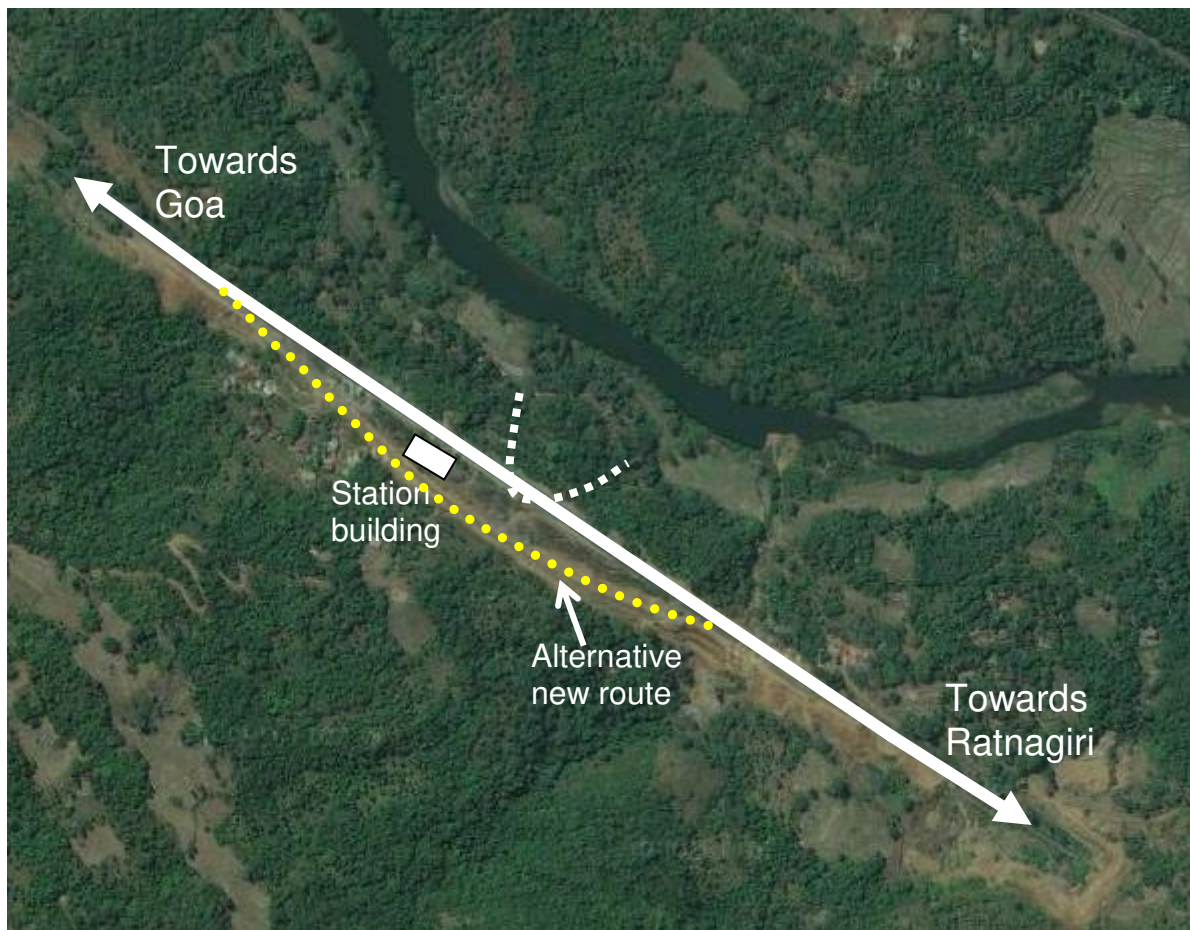


Figure 1. Nivsar Station in Ratnagiri District of Maharashtra (Source: Google earth). Note: The dashed line shows the approximate location of the embankment failure .

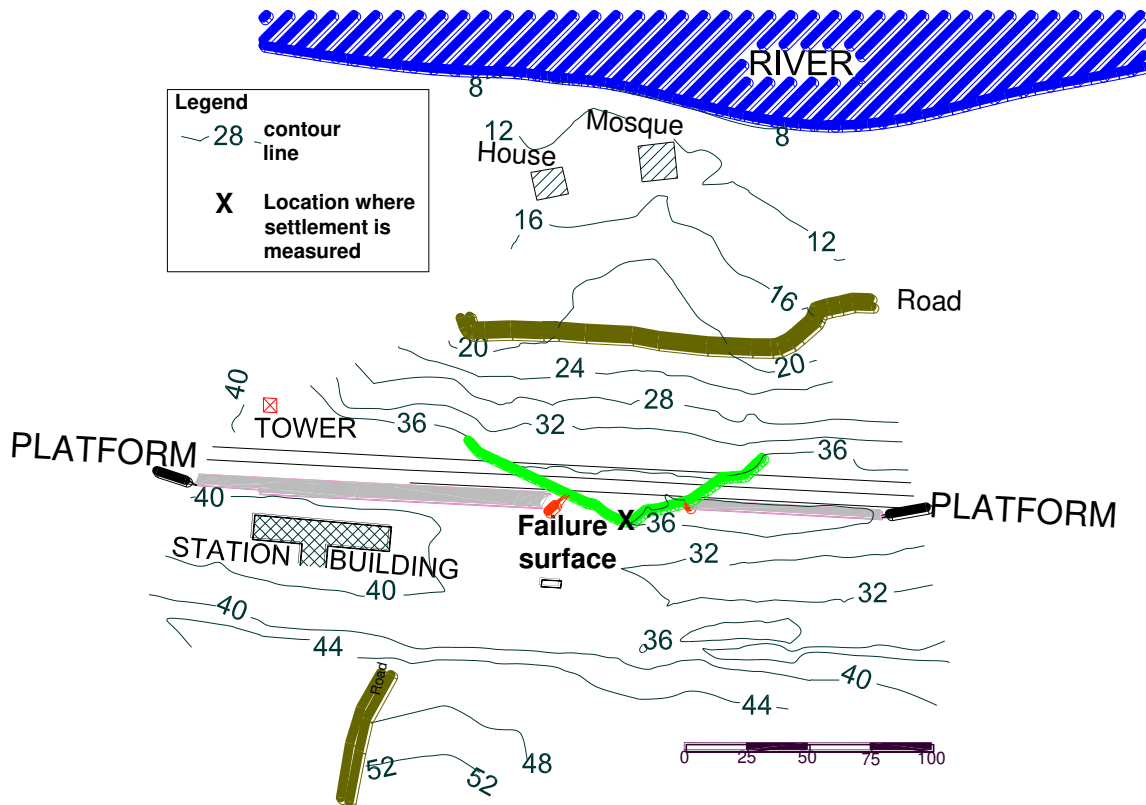


Figure 2. Failure at Nivsar Yard Embankment

Immediately after the 2006 monsoon season, the space beneath the ballast of the main and loop lines was filled with cement grout. Table 1 also shows details of the ground improvement works undertaken after the monsoon in January 2007. During the remainder of that year, the embankment did not deform. However during the 2008 monsoon, cracks redeveloped and were similar to those that appeared following the 2005 and 2006 monsoons. During this time, the settlement reached a maximum of 215mm at the platform edge. Ground remedial works were again carried out during January 2009. Table 2 shows the total cement consumed during the 2009 and 2007 grouting process. Despite the above measures undertaken to improve the stability, the slope settled again during the 2009 monsoon. This time the total settlement was close to its original level, reaching 2990mm at the station platform. The failure resulted in severe disruption of the rail traffic. Unfortunately, the failure surface again reappeared during the 2010 monsoon. This happened even as several relief wells were in operation on top of the embankment. From 05/06/10 to 26/07/10, i.e., within a period of two months, the embankment settled by more than 2170mm. The settlement stopped during the first week of October 2010, when the monsoon was over. By that time, the embankment had settled by 2290mm at the station platform.

Figure 3 shows the recorded settlement of the embankment from the year 2005. The settlement was measured at top of the embankment near the station platform and its location is shown in Figure 2. Figure 3 also shows the record of rainfall in this region. The rainfall record was obtained from the web pages of <http://www.wunderground.com/> and from the data maintained by Konkan Railways. A clear trend between the magnitude of rainfall and slope movement can be observed in Figure 3. For instance, rainfall of over 200mm per day was invariably followed by more than 100mm settlement every year except during the 2007 and 2008 monsoons. The embankment did not move during the 2007 monsoon. Movement occurred only after more than half of the 2008 monsoon was complete. It appears that the stabilisation work completed before the onset of the 2007 monsoon was insufficient and effective only for a year, before losing effectiveness during the 2008 monsoon. It is likely that the slip planes redeveloped along the original failure surface during the 2008 ground failure. All effects of the soil improvement vanished before the onset of the 2009 monsoon, resulting in rapid movement of the embankment towards the river. The failure cracks that developed in 2009 are shown in Figures 4a-c. Figures 4a and b show the top few meters of the micro-piles that were exposed because of the steady soil-flow down the hill, and Figure 4c shows the transverse cracks observed along the road.



*Table 1. Ground improvement measures at Nivsar Yard Embankment since 2005*

| Period        | Ground Improvement Measures  |
|---------------|--|
| November 2005 | <ol style="list-style-type: none"> <li>Seven rows of 76 to 89mm-diameter soil nails were installed at 1.5m centre to centre and up to 15m depth, along the east and the west side of the embankment.</li> <li>One row of 200mm diameter micropiles were installed for 105m length at 1.5m centre to centre and up to 15m depth, along the east side of the embankment.</li> <li>Two rows of 200mm diameter micropiles were installed for 160m length at 1m centre to centre and up to 15m depth, along the west side and on first berm.</li> <li>One row of 300mm diameter micropiles were installed for 160m length at 1.5m centre to centre and up to 10m depth, along the east side of the embankment.</li> </ol>   |
| August 2006   | Four relief wells were installed at uphill side. About 4.4 million litres of water were removed from these wells in August and September 2006.   |
| January 2007  | <ol style="list-style-type: none"> <li>Five rows of grout curtains were installed at 3m centre to centre and up to 20m depth, for 105m length at uphill side and for 160m length at downhill side.</li> <li>Twenty rows of consolidation grouting works were conducted at 3m centre to centre and up to 18m depth at uphill side.</li> <li>Two rows of 300mm diameter micropiles were installed for 160m length at 1.5m centre to centre and up to 36m depth, along the west side between the previous two rows.</li> <li>Two rows of 300mm diameter micropiles were installed at 1m centre to centre and up to 28 to 35m depth.</li> <li>One row of 76mm diameter GI pipe drains wrapped with geotextile filter were installed at 2m centre to centre at 15 degrees to vertical and up to 6m depth along the west side berm.</li> </ol> |
| August 2007   | The relief wells installed in 2006 were operational from August to September 2007.   |
| January 2009  | Grout curtains and consolidation grouting works were conducted on the embankment. Additional relief wells were installed making a total of 7 wells on the uphill side.   |
| June 2009     | All 7 relief wells were operational during the 2009 monsoon.   |
| June 2010     | Relief wells were operational during the 2010 monsoon.   |

*Table 2. Total cement used in grouting*

| Year | Location                  | Cement consumption: kg |
|------|---------------------------|------------------------|
| 2007 | Uphill curtain grouting   | 101,800                |
|      | Downhill curtain grouting | 95,550                 |
|      | Consolidation grouting    | 1,901,150              |
|      | Micro-piling              | 317,400                |
|      | Pile cap                  | 79,350                 |
| 2009 | Uphill curtain grouting   | 21,550                 |
|      | Consolidation grouting    | 287,750                |

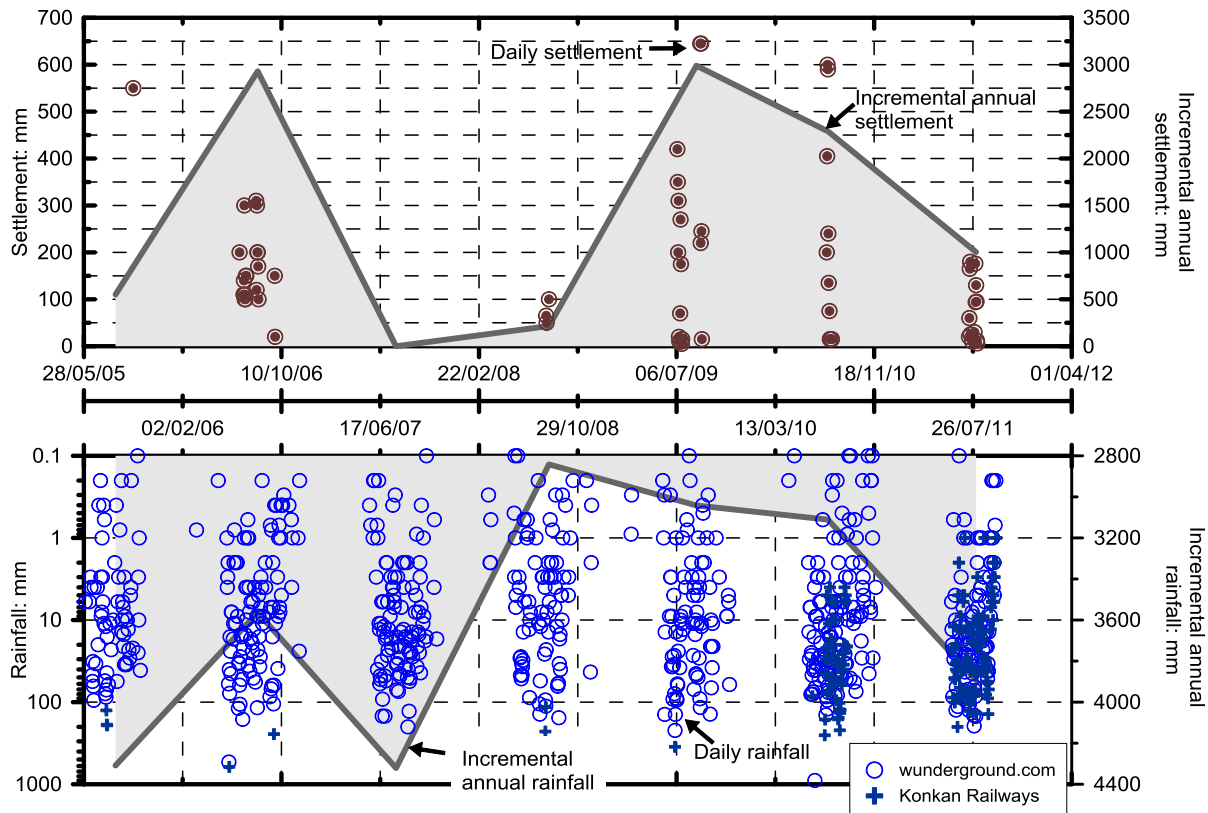


Figure 3. Settlement and rainfall record at Nivsar Yard Embankment.

Figure 5 shows the map of the failure surface at the Nivsar Yard Station. In the figure, the latitudes and longitudes were obtained from the local coordinates using the WGS84 method (Chen and Hill 2005). The location of the slump, transverse cracks, and the failure surface are marked in the figure. The position of the transverse cracks was obtained by superimposing the observations made in Figure 4c onto Figure 5. All of the above, and the location of slope-reversal and scarp shown by the tilted trees and the cracked brick walls in Figure 6, suggest that they are parts of a landslide event.

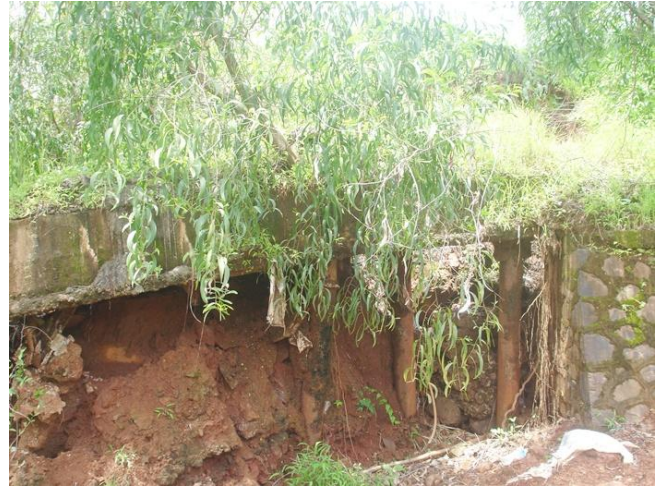
In 2010, the rail track was realigned to bypass the failure surface. This arrangement provided immediate relief to the rail-traffic. Figure 1 also shows the new alternate route used by the Konkan Railways. Since then, three other lines have been realigned to follow this alternate route. Irrespective of the above change in the rail alignment, Figure 3 also shows that the rate of settlement of the embankment has reduced since the 2009 monsoon. It is plausible to assume that the slump accumulated at the toe has reduced the gradient and hence affected the soil movement over this period (Figure 5). The site was re-investigated in 2010. The results of the re-investigation are part of this present study. The objective of this paper is to investigate the slope failure at Nivsar as recorded since the year 2005. Stability of the embankment before and after the ground improvement works is discussed. Railway loads from the old as well as the new rail alignment were used in the analysis. The critical failure circle for each case is shown to be affected by the geometry of the slope and the hydrogeological conditions at the site.

### SITE GEOLOGY AND GEOTECHNICAL PROPERTIES

The soils and rocks at Ratnagiri district belong to the following five main groups: (1) Archaean deposits; (2) Basalt trap; (3) Ratnagiri plant beds; (4) Konkan laterite; and (5) Ratnagiri alluvial. Details of these deposits are available by the Geological Survey of India (Singh 2010) and are summarised below.



(a)



(b)



(c)

*Figures 4a-c. Failure of micropiles and curtain grouting: (a) and (b) Exposed pile foundation; and (c) Location of transverse cracks along the road (curtain grouting was conducted around this location).*

**Archaean Deposits:** Archaean deposits are the oldest metamorphic rocks in the Ratnagiri district. The origin of these rocks was affected by lineaments (faults) that transverse parallel to the west coast. Archaean rocks are mostly covered by the volcanic (Basalt) traps and the Konkan laterites. At some locations, these rocks are exposed at the surface and exist as islands surrounded by the volcanic traps. Along the Ratnagiri coast, these metamorphic rocks occur as thin bands of gneiss and mica schists. Quartz and shales can also be observed further south of this region. Shales occur as pockets within the lower sandstone beds.

**Basalt Trap:** Basalt trap were formed from volcanic eruption and are black to greenish-grey in colour. The flow from the volcanic outburst probably originated deep inland, far away from the Konkan coast because the rock has a seaward dip with visible flow lines. The trap is about 1000m thick near the coast and substantially thicker inland. Basalt traps are covered by thick laterite beds which may otherwise exist as exposed patches beyond the Ratnagiri district.



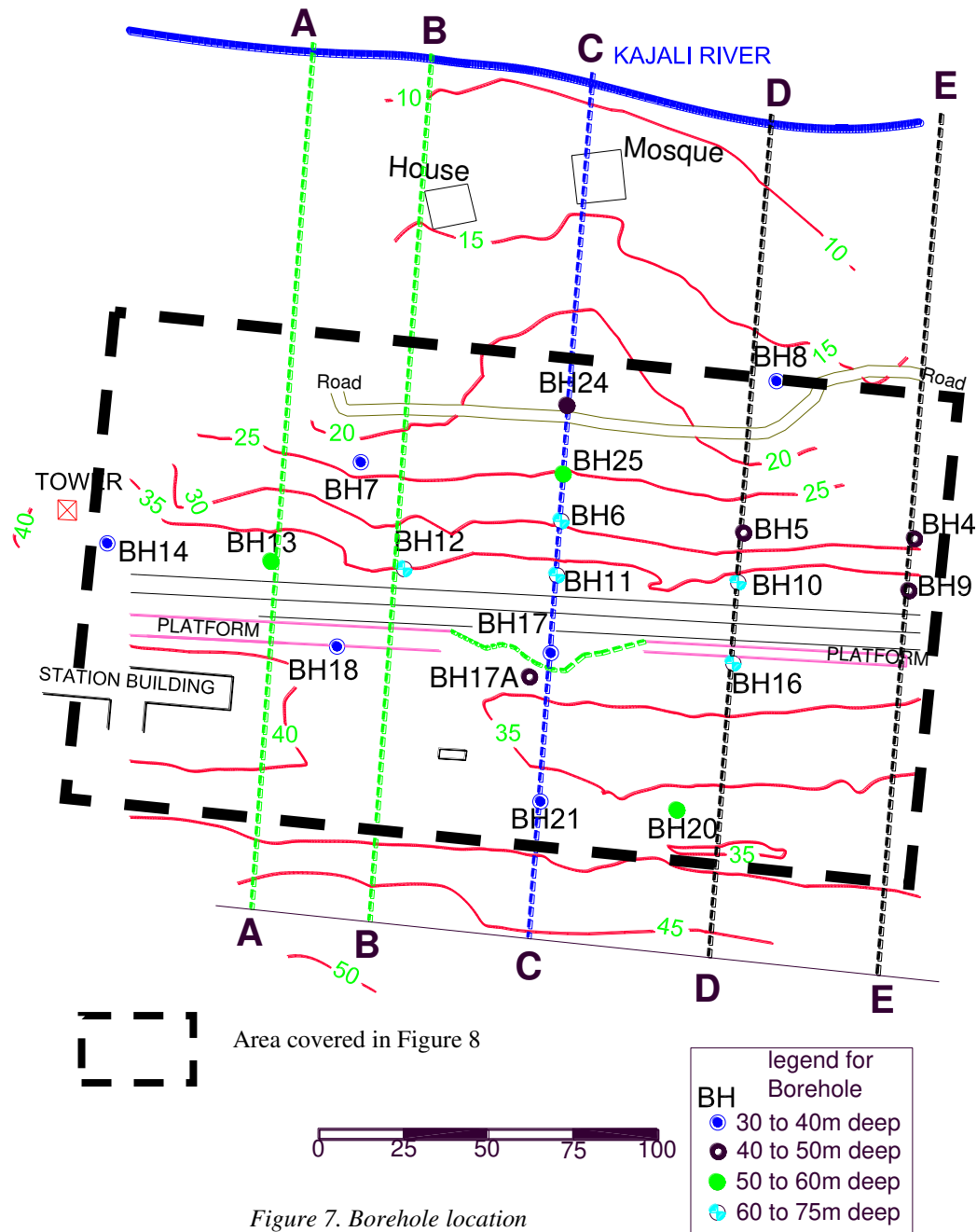


Figure 7. Borehole location

**Ratnagiri Alluvial:** Ratnagiri alluvial consist of silts and sands deposited at the lower reaches of the river. Properties of the alluvial depend almost entirely on the properties of the parent rock and the mode of transportation. Close to the delta, these deposits are stiff when mixed with broken shell pieces. Otherwise, alluvial above the high water mark are covered by Aeolian soils.

#### GEOTECHNICAL PROFILE AT THE SITE

Geotechnical data was collected from 19 boreholes drilled at the top and bottom of the embankment. These boreholes were drilled in the year 2010. Figure 7 shows the location of the boreholes. All boreholes, except for BH-20 and BH-21, were



drilled at the location of the failure. These two boreholes were located near the new alignment. Boreholes BH17 and 17A were drilled adjacent to the vertex of the failure surface; while care was taken to drill all other boreholes through the undisturbed zone. Many boreholes were of 50m depth. However, some boreholes were drilled deeper to over 60m depth at locations where the rock mass was highly fractured. Table 3 summarises the thicknesses of the soil and rock layers in each borehole. Using the data presented in the table, the 3-dimensional cross-section of the subsurface profile shown in Figure 8 was developed. A brief description of the layers in this profile is presented below. This description follows the order in which the layers were encountered in the boreholes.

*Table 3. Thickness of the soil/ rock strata and their depth below surface in each borehole*

| Borehole ID | Depth of the layer (m) |               |              |              | Depth of slightly to moderately weathered Basalt (m) | Total borehole depth (m) |
|-------------|------------------------|---------------|--------------|--------------|--|--------------------------|
|             | Fill                   | Residual soil | Laterite     | Basalt       |  |                          |
| BH-04       | 0 to 10.5              | 10.5 to 15    | 15 to 36     | 36 onwards   | 45   | 46                       |
| BH-05       | 0 to 12                | 12 to 19.5    | 19.5 to 34.5 | 34.5 onwards | 42   | 45                       |
| BH-06       | 0 to 13.5              | 13.5 to 27    | 27 to 34.5   | 34.5 onwards | 46.5   | 61.5                     |
| BH-07       | 0 to 10                | -             | 10 to 13     | 13 onwards   | 17.5   | 30                       |
| BH-08       | -                      | 0 to 19.5     | 19.5 to 21   | 21 onwards   | 25.5   | 30                       |
| BH-09       | 0 to 16.5              | 16.5 to 28.5  | 28.5 to 42   | 42 onwards   | 46.5   | 46.5                     |
| BH-10       | 0 to 15                | 15 to 25      | 25 to 49.5   | 49.5 onwards | 54   | 65                       |
| BH-11       | 0 to 15                | 15 to 27      | 27 to 46     | 46 onwards   | 49   | 75                       |
| BH-12       | 0 to 13.5              | 13.5 to 21    | 21 to 45     | 45 onwards   | 51   | 75                       |
| BH-13       | 0 to 4.5               | 4.5 to 16     | 16 to 19     | 19 onwards   | 34   | 52                       |
| BH-14       | 0 to 6                 | 6 to 19.5     | 19.5 to 22.5 | 22.5 onwards | 22.5   | 30                       |
| BH-16       | 0 to 4.5               | 4.5 to 19.5   | 19.5 to 42   | 42 onwards   | 42   | 75                       |
| BH-17       | 0 to 9                 | 9 to 20       | 20 to 24.5   | 24.5 onwards | 28.5   | 32                       |
| BH-17A      | 0 to 9                 | 9 to 21       | 21 to 22.5   | 22.5 onwards | 25.5   | 40                       |
| BH-18       | 0 to 1.5               | 1.5 to 17.5   | -            | 17.5 onwards | 17.5   | 30                       |
| BH-20       | 0 to 6                 | 6 to 9        | 9 to 38.5    | 38.5 onwards | 40   | 50                       |
| BH-21       | 0 to 4.5               | 4.5 to 15     | -            | 15 onwards   | 16.5   | 33                       |
| BH-24       | -                      | 0 to 18       | 18 to 24     | 24 onwards   | 28.5   | 42                       |
| BH-25       | 0 to 9                 | 9 to 18       | 18 to 36     | 36 onwards   | 40   | 50                       |

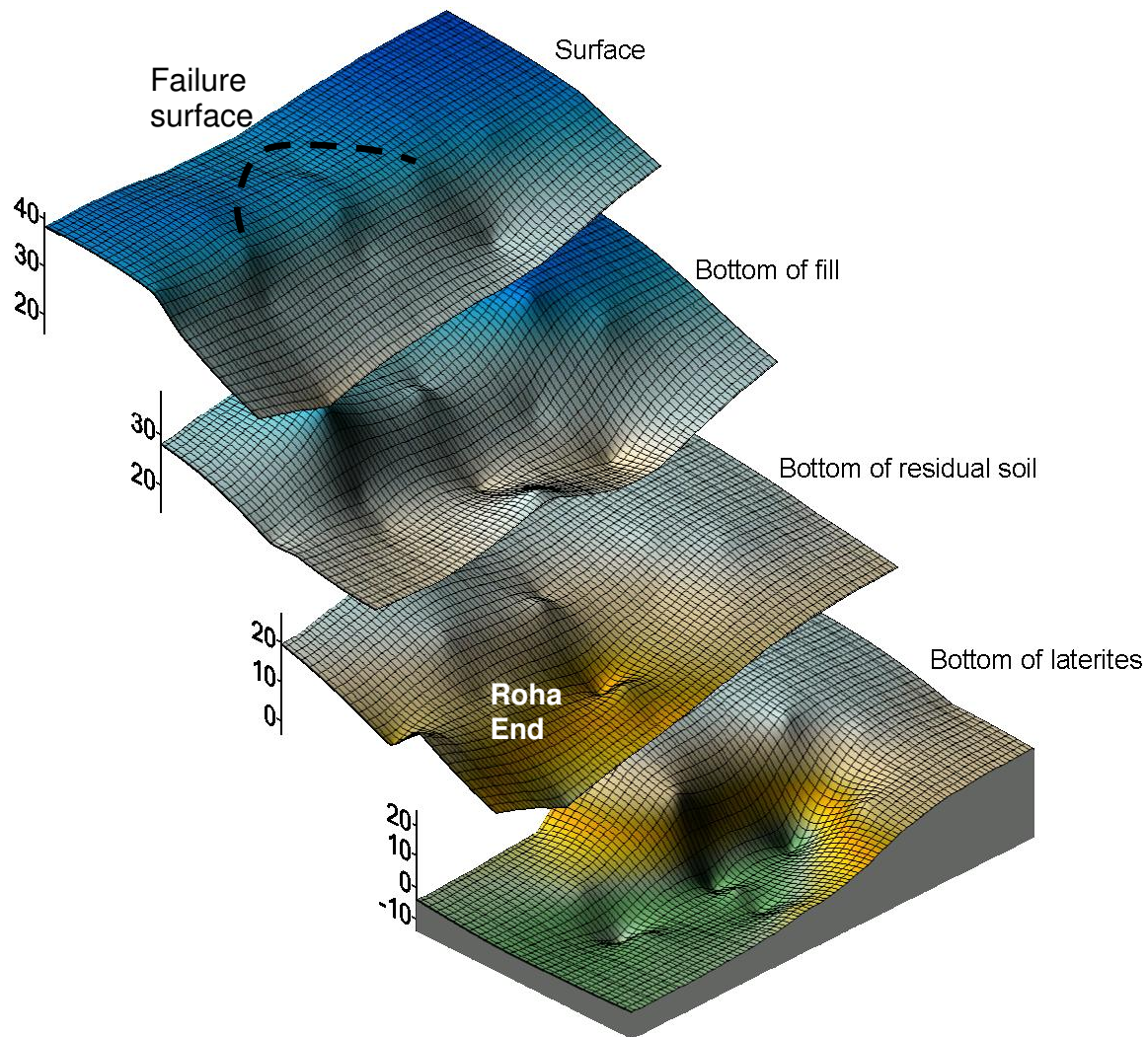


*Figure 8. Three dimensional cross-sections of the soil and rock layers*

**Fill:** Fill consisted of reddish brown silty clay and clayey sand. The clay matrix was frequently filled with coarse gravel and cobbles, which made this topmost-soil-layer firm to stiff. The fill was classified as medium to dense at locations where the sand and gravel proportions were in majority. The thickness of the fill was in between 13.5 to 15m in boreholes drilled close to the rail line at top of the hill. The thickness of the fill was surprisingly only 9m in borehole BH-17 drilled near the vertex of the failure surface. Apparently, the slip along the failure surface had caused the fill thickness to reduce at this location. The fill gradually narrowed towards the top flat end of the hilltop. Likewise, boreholes BH-7, BH-8, BH-24 and BH-24 indicate that the fill tapered off downhill at the road level. Figure 8 shows that the fill is bowl-shaped with its edges fused to the edges of the section. From Figure 8, it is interesting to note that the shape of the failure surface mimics the shape of the fill.

**Residual soil:** Residual soil consisted of reddish brown clayey sand and sandy/silty clay with gravel. The gravel content varied considerably and controlled the penetration resistance in many boreholes. Residual soils extended till 9.3m to 28.5m below the surface. Thickness of the residual soils was more than 10m except in boreholes BH-4, BH-5, BH-7, BH-12, BH-20 and BH-25. Figure 8 shows that the base of the residual soils sloped towards the Roha End. Residual soils were medium-dense to dense when the soils were coarse-grained or were soft and stiff when the soils were fine grained. In general, these soils had better consistency and improved compaction compared to the fill.



**Laterite rock:** Laterites were logged from 9.3m to 28.5m below surface. Thickness of the laterites was over 20m in boreholes BH-4, BH-10, BH-12, BH-16 and BH-20. Most laterites were fractured and crumbled when soaked. However, in a dry state the unconfined compressive strength (UCS) of the laterites was reasonably high, varying between 400 and 5600 kN/m<sup>2</sup>. Rock Quality Designation (RQD) was mostly zero although the core recovery was 100%.

**Basalt bedrock:** Basalt bedrock was logged from 13m to 49.5m below ground surface. As shown in Figure 8, the top surface of the basalt was undulating which provided a strong grip to the above laterites. The bedrock was weathered at the top with fractures at many locations. The depth from which the quality of the basalt improved to slightly/moderately weathered is shown in Table 3. The UCS of the bedrock was in between 200 kN/m<sup>2</sup> and 124 MN/m<sup>2</sup>. Table 3 also shows the termination depth in each borehole.

Using the borehole data, five cross-sections were drawn to interpret the subsurface profile of the site. The five sections are marked as A-A to E-E in Figure 7 and are shown in Figure 9. Sections B-B to D-D were chosen to represent the edges and centre of the failure zone. Laterites were nearly absent in section A-A and had the maximum presence in section D-D. The average geotechnical properties at each section are shown in Table 4. The material properties in Table 4 were obtained from the field and laboratory testing programme monitored jointly by Konkan Railways and IIT Bombay. Direct shear tests were conducted to obtain  $c'$  and  $\phi'$ . Unconsolidated undrained (UU) triaxial tests were conducted to obtain  $c_u$ . The secant Young's modulus,  $E$ , of selected samples was obtained from stress-strain curves on UU samples confined with 50 to 200 kN/m<sup>2</sup> mean stress. Unconfined compression tests were conducted to obtain the  $c_u$  of laterites and basalt.

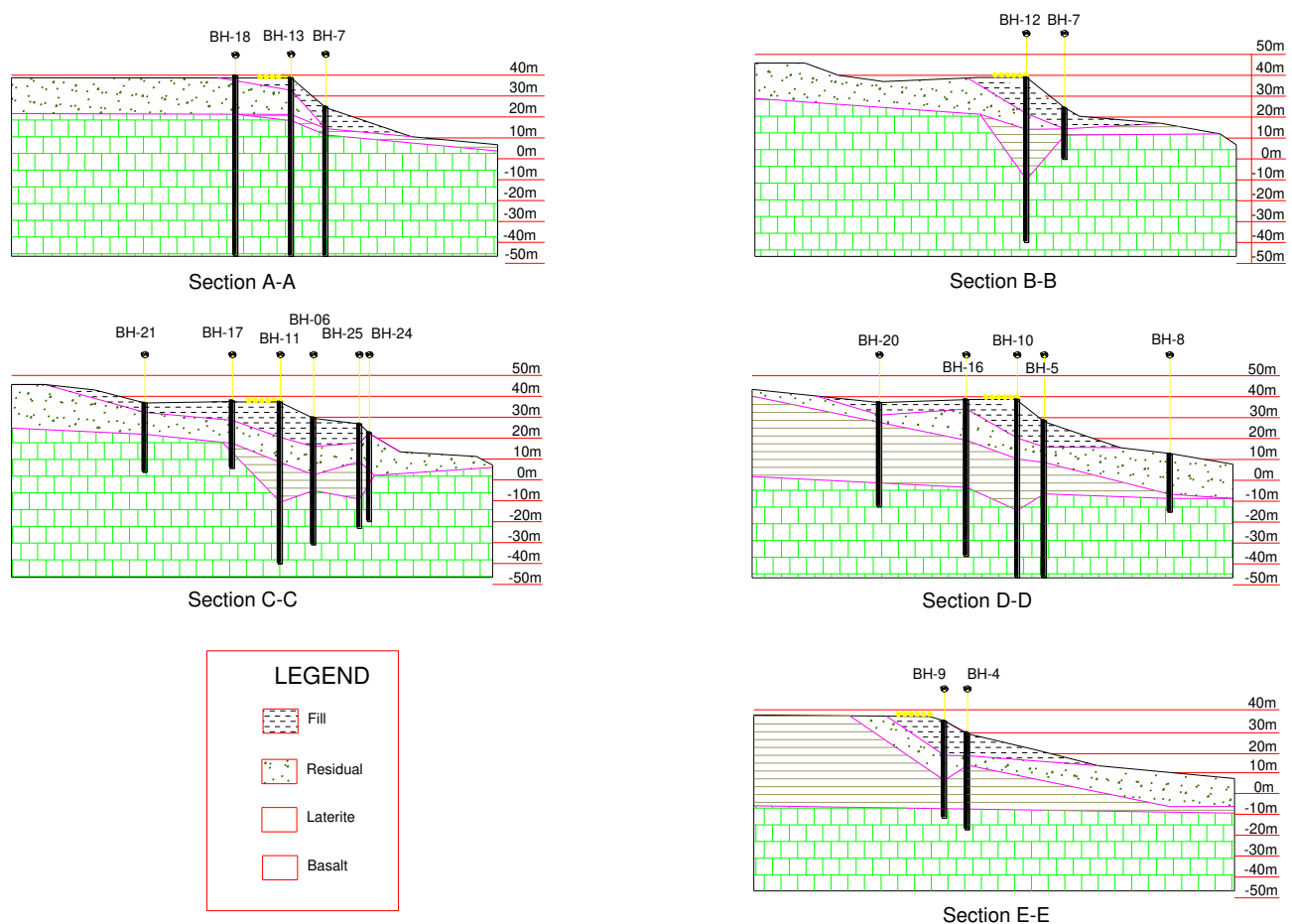


Figure 9. Subsurface profile at the site. Location of sections A-A to E-E are as per Figure 7.



Standpipes were installed in the boreholes after the completion of the drilling. Ground water depths were occasionally recorded in these standpipes for about two years. Figures 10a and 10b show the water table recorded in 2010 and 2011, respectively. The slope movement during the 2010 and 2011 monsoons, sheared-off some of the standpipes. As a result a complete record of ground water data is not available over the monitoring period at these locations. The maximum and minimum water table depths are summarised in Table 5. A few observations may be made from Figures 10a-b and Table 5. First, the water table changed from 12.5m to 20m over the monitoring period in boreholes which were drilled along the centre-line of the failure surface. This variation in the water level possibly created a large pressure gradient. Second, the seasonal variation in the water level was more than 9m in boreholes drilled within the failure zone. There was significant variation in the water level even outside the failure surface. For example, the pressure head difference between boreholes BH-7 and BH-12 was more than 17m although the boreholes were only about 35m apart. Inevitably, these large pressure head difference caused large groundwater flow and significant seepage forces.

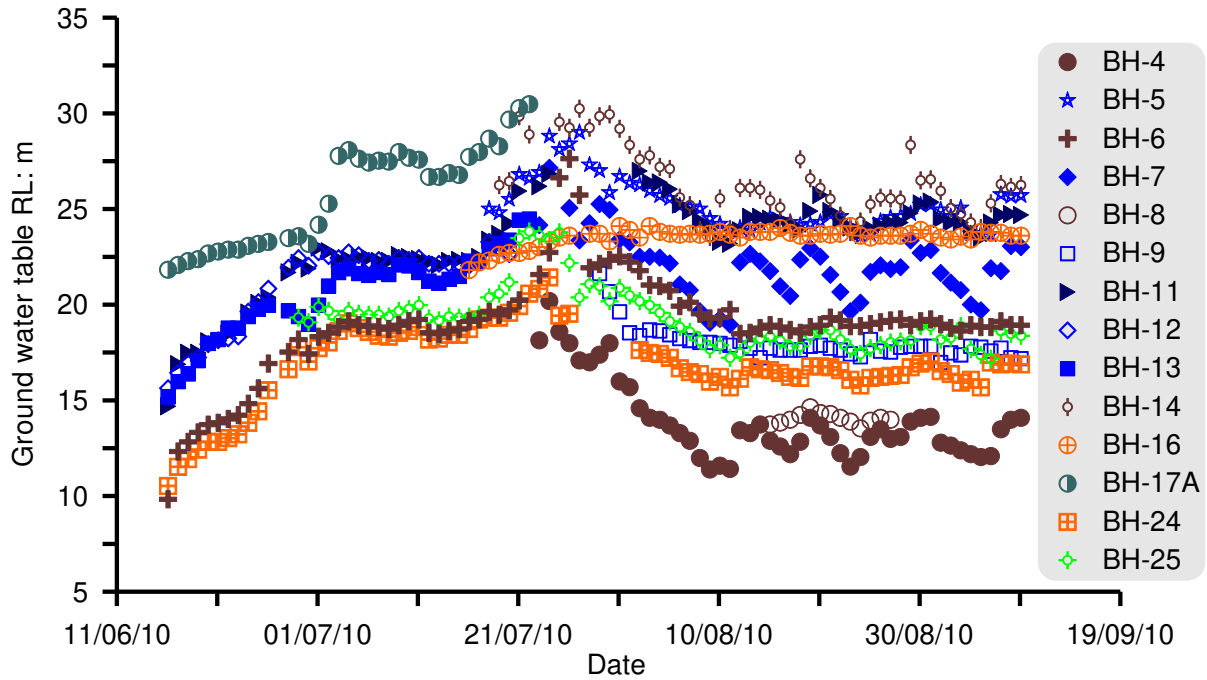
Table 4. Average geotechnical properties at each section

| Section | Strata Type | SPT N | Sand % | Passing # 200 sieve % | LL % | PL % | c' kN/m <sup>2</sup> | $\phi^0$ | c <sub>u</sub> kN/m <sup>2</sup> | $\phi_u^0$ | $\gamma_{bulk}$ kN/m <sup>3</sup> | $\gamma_{dry}$ kN/m <sup>3</sup> | $\gamma_{solids}$ kN/m <sup>3</sup> | E kN/m <sup>2</sup> | d <sub>50</sub> mm |
|---------|-------------|-------|--------|-----------------------|------|------|----------------------|----------|----------------------------------|------------|-----------------------------------|----------------------------------|-------------------------------------|---------------------|--------------------|
| A-A     | Fill        | 13    | 30     | 29                    | 47   | 23   | 9.81                 | 19       | -                                | -          | 17.07                             | 11.77                            | 25.95                               | 9                   | 0.31               |
|         | Residual    | 28    | 33     | 41                    | 44   | 24   | 17.46                | 24       | 64.75                            | 3          | 17.57                             | 13.24                            | 26                                  | 19                  | 0.63               |
|         | Laterite    | -     | -      | -                     | -    | -    | -                    | -        | 20554                            | -          | -                                 | 24.69                            | -                                   | 1630                | -                  |
|         | Basalt      | -     | -      | -                     | -    | -    | -                    | -        | 25324                            | -          | -                                 | 27.19                            | -                                   | 2603                | -                  |
| B-B     | Fill        | 16    | 36     | 43                    | 39   | 22   | 14.23                | 19       | -                                | -          | 17.07                             | 11.82                            | 26                                  | 11                  | 0.44               |
|         | Residual    | 32    | 47     | 35                    | 47   | 23   | 14.72                | 29       | -                                | -          | 17.86                             | 13.07                            | 26                                  | 17                  | 0.9                |
|         | Laterite    | -     | -      | -                     | -    | -    | -                    | -        | 12283                            | -          | -                                 | 18.89                            | -                                   | 1166                | -                  |
|         | Basalt      | -     | -      | -                     | -    | -    | -                    | -        | 27155                            | -          | -                                 | 28.27                            | -                                   | 2592                | -                  |
| C-C     | Fill        | 18    | 29     | 34                    | 42   | 23   | 15.3                 | 28       | -                                | -          | 17.8                              | 13.13                            | 26.01                               | 21                  | 1.37               |
|         | Residual    | 24    | 33     | 46                    | 51   | 24   | 14.47                | 29       | 54.45                            | 3          | 17.82                             | 13.18                            | 26.01                               | 25                  | 1.16               |
|         | Laterite    | -     | -      | -                     | -    | -    | -                    | -        | 4454                             | -          | -                                 | 18.67                            | -                                   | 1214                | -                  |
|         | Basalt      | -     | -      | -                     | -    | -    | -                    | -        | 21090                            | -          | -                                 | 26.96                            | -                                   | 2120                | -                  |
| D-D     | Fill        | 15    | 36     | 40                    | 43   | 23   | 17.98                | 19       | 83.39                            | 2.6        | 17.73                             | 13.05                            | 26.01                               | 13                  | 0.57               |
|         | Residual    | 25    | 23     | 55                    | 44   | 24   | 15.21                | 24       | -                                | -          | 17.17                             | 12.04                            | 26.01                               | 24                  | 0.29               |
|         | Laterite    | -     | -      | -                     | -    | -    | -                    | -        | 2071                             | -          | -                                 | 20.61                            | -                                   | 1286                | -                  |
|         | Basalt      | -     | -      | -                     | -    | -    | -                    | -        | 27810                            | -          | -                                 | 26.89                            | -                                   | 1870                | -                  |
| E-E     | Fill        | 30    | 20     | 47                    | 41   | 22   | 17.66                | 29       | -                                | -          | 17.22                             | 12.21                            | 26.09                               | 39                  | 1.32               |
|         | Residual    | 40    | 38     | 55                    | 54   | 27   | 18.64                | 24       | -                                | -          | 17.1                              | 11.87                            | 26.02                               | 36                  | 0.3                |
|         | Laterite    | -     | -      | -                     | -    | -    | -                    | -        | 5608                             | -          | -                                 | 20.37                            | -                                   | 1259                | -                  |
|         | Basalt      | -     | -      | -                     | -    | -    | -                    | -        | 12346                            | -          | -                                 | 22.94                            | -                                   | 2851                | -                  |

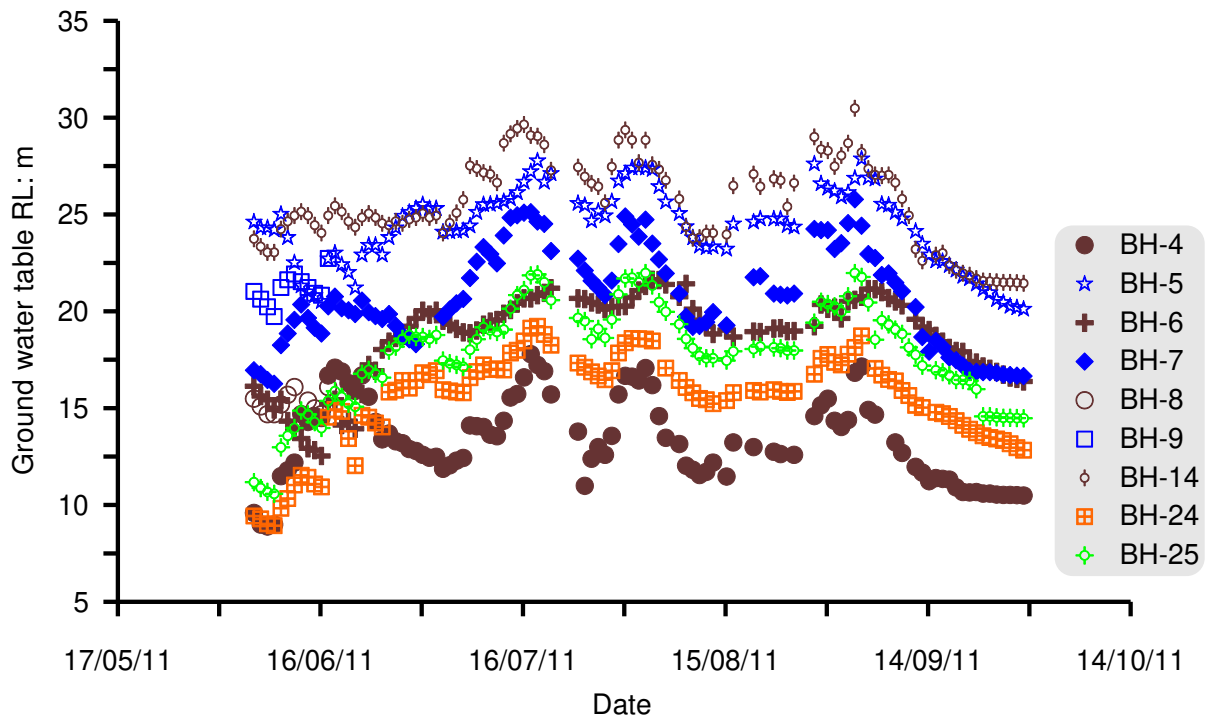
## SLOPE STABILITY ANALYSIS

### SLOPE FAILURE IN 2005

Failure of the slope in 2005 was investigated using the upper bound limit equilibrium method. In this method, the safety factor was calculated by assuming that the block of sliding mass was in the state of plastic equilibrium. The analysis was done using the Simplified Bishop method. This approach was chosen in lieu of the more rigorous displacement based procedures because this method is shown to give reasonably accurate results for most cases with the least computational effort (Spencer 1967). A uniformly distributed live load of 125 kN/m<sup>2</sup> was used for the design axle and track loads. The axle load included the impact-factor at the track level for equivalent heavy mineral loading (RDSO 2003a). Because of the single-track Konkan Railway, Nivsar station had 2 passing loops in 2005. Because the passing loops were often used for overtaking of freight trains, all 3 sets of tracks were assumed to carry the full railway load, spread over 3m width at the foundation level.



(a)



(b)

Figures 10a-b. Water table in standpipes: (a) In 2010; and (b) In 2011.

Note: Reduced level (RL) was deduced from the datum located at the platform level.



*Table 5. Ground water table observations in the boreholes*

| Borehole | Borehole RL | Month of investigation | GWT at time of investigation | Max RL in 2010 and 2011 | Min RL in 2010 and 2011 | Difference in water level |
|----------|-------------|------------------------|------------------------------|-------------------------|-------------------------|---------------------------|
| BH 4     | 29.84       | July                   | 17.74                        | 20.24                   | 8.24                    | 12                        |
| BH 5     | 28.576      | July                   | 22.226                       | 28.06                   | 20.162                  | 8.898                     |
| BH 6     | 29.428      | May                    | 18.428                       | 27.68                   | 9.88                    | 17.8                      |
| BH 7     | 24.407      | July                   | 2.207                        | 24.21                   | 16.307                  | 25.003                    |
| BH 8     | 15.92       | August                 | 7.62                         | 15.14                   | 13.59                   | 8.52                      |
| BH 9     | 35.686      | July                   | 17.686                       | 22.782                  | 17.03                   | 5.752                     |
| BH 10    | 35.199      | March                  | 7.349                        | -                       | -                       | -                         |
| BH 11    | 35.34       | May                    | 7.24                         | 27.04                   | 14.74                   | 19.8                      |
| BH 12    | 35.133      |                        | -                            | 23.34                   | 15.69                   | 7.65                      |
| BH 13    | 37.032      | May                    | 8.532                        | 24.53                   | 15.23                   | 15.998                    |
| BH 14    | 38.308      | July                   | 26.808                       | 30.537                  | 21.497                  | 9.04                      |
| BH 16    | 38.633      | April                  | 14.833                       | 24.16                   | 21.86                   | 9.327                     |
| BH 17    | 37.491      | April                  | 13.991                       | -                       | -                       | -                         |
| BH 17A   | 36.289      | May                    | 12.689                       | 30.53                   | 21.88                   | 17.841                    |
| BH 18    | 38.8        | June                   | 26                           | -                       | -                       | -                         |
| BH 20    | 37.201      | April                  | 17.101                       | -                       | -                       | -                         |
| BH 21    | 37.042      | April                  | 16.642                       | -                       | -                       | -                         |
| BH 24    | 22.082      | May                    | 10.082                       | 21.48                   | 8.982                   | 12.498                    |
| BH 25    | 26.778      | June                   | 14.978                       | 23.88                   | 10.627                  | 13.253                    |

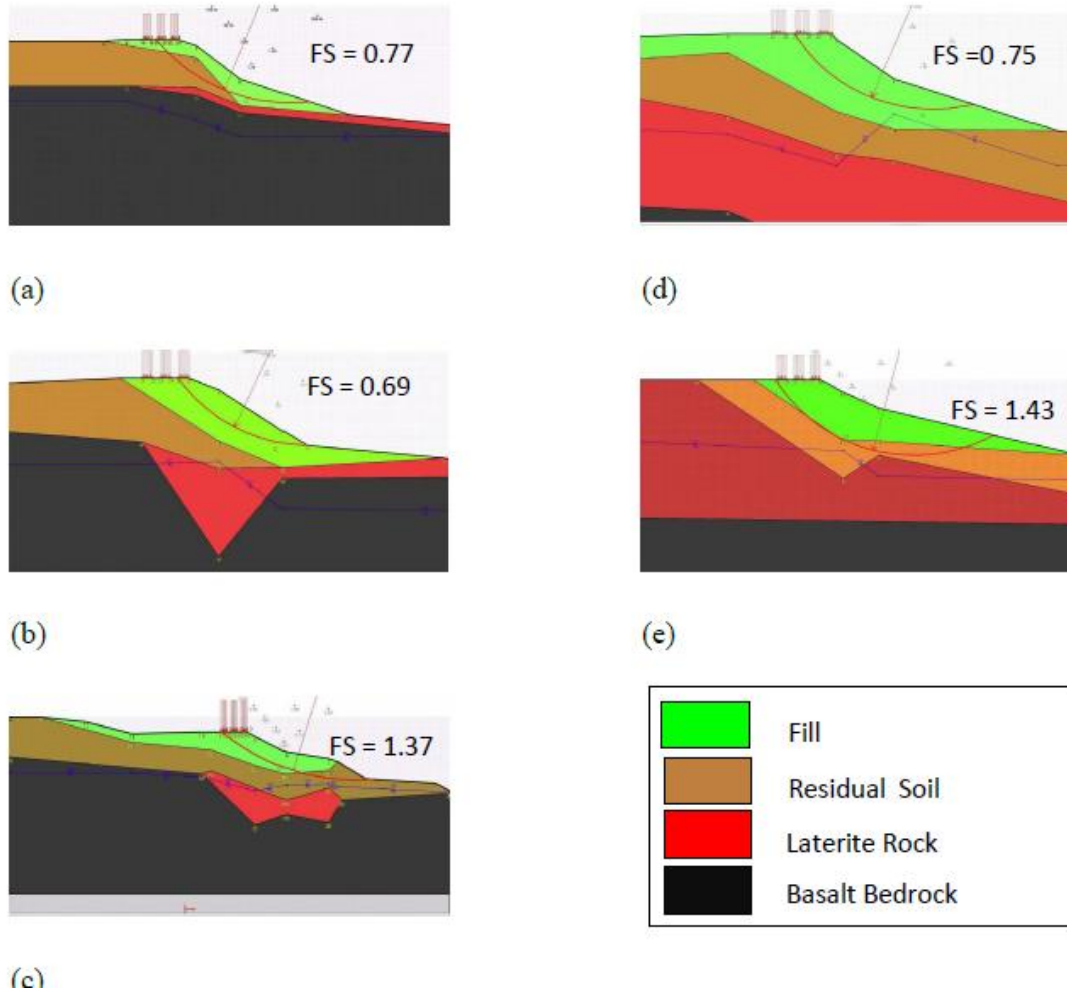
Note: Monsoon period is mid-June to end of September; all numeric values are in meters

Geotechnical properties of the slope prior to the 2005 failure were not available. It was therefore prudent to use the properties of the soil and rock from Table 4. Similarly, the hydrological properties were taken from Table 5. Calculations were done using the commercial program Talren-4 (Terrasol 2005). The program permitted the soil to deform and develop pore pressure above the slip surface. The imposed failure circles were set at the interface of the fill and the residual soils. In the analysis, the circular failure surface was divided into 150 slices and the search type was set to automatic. This setting searches for the most critical circle at 0.25m intervals. In essence, the procedure used to determine the slope stability was as follows:

1. The stability of sections A-A to E-E along with the imposed railway loading was calculated using the lowest ground water table elevation. This step yielded the safety factor during the dry season.
2. The stability of sections A-A to E-E with the railway loading was calculated using the highest ground water table elevation. This step yielded the safety factor during the monsoon season.
3. The safety factors obtained in Steps 1 and 2 were compared to obtain the minimum safety factor for all failure surfaces.



Figures 11a-e show the minimum safety factor and the location of the critical circle in sections A-A to E-E for the dry season. It is surprising to note that the minimum safety factor in 3 out of 4 sections is less than one, despite the fact that the slope was known to be stable and did not show any distress during the dry season. These sections are A-A, B-B and D-D in the figures. Figures 11a to 11e also show that the ground water level is below the critical failure circle in all 4 cases. Therefore, even if it is argued that the hydrological conditions which led to the 2005 failure and those measured in 2010 and 2011 may not be the same, it is unlikely that the position of the water table could influence the stability of the slope during the dry season.



Figures 11a-e. Safety factor during dry season with original parameters for section: (a) A-A; (b) B-B; (c) C-C; (d) D-D; and (e) E-E.

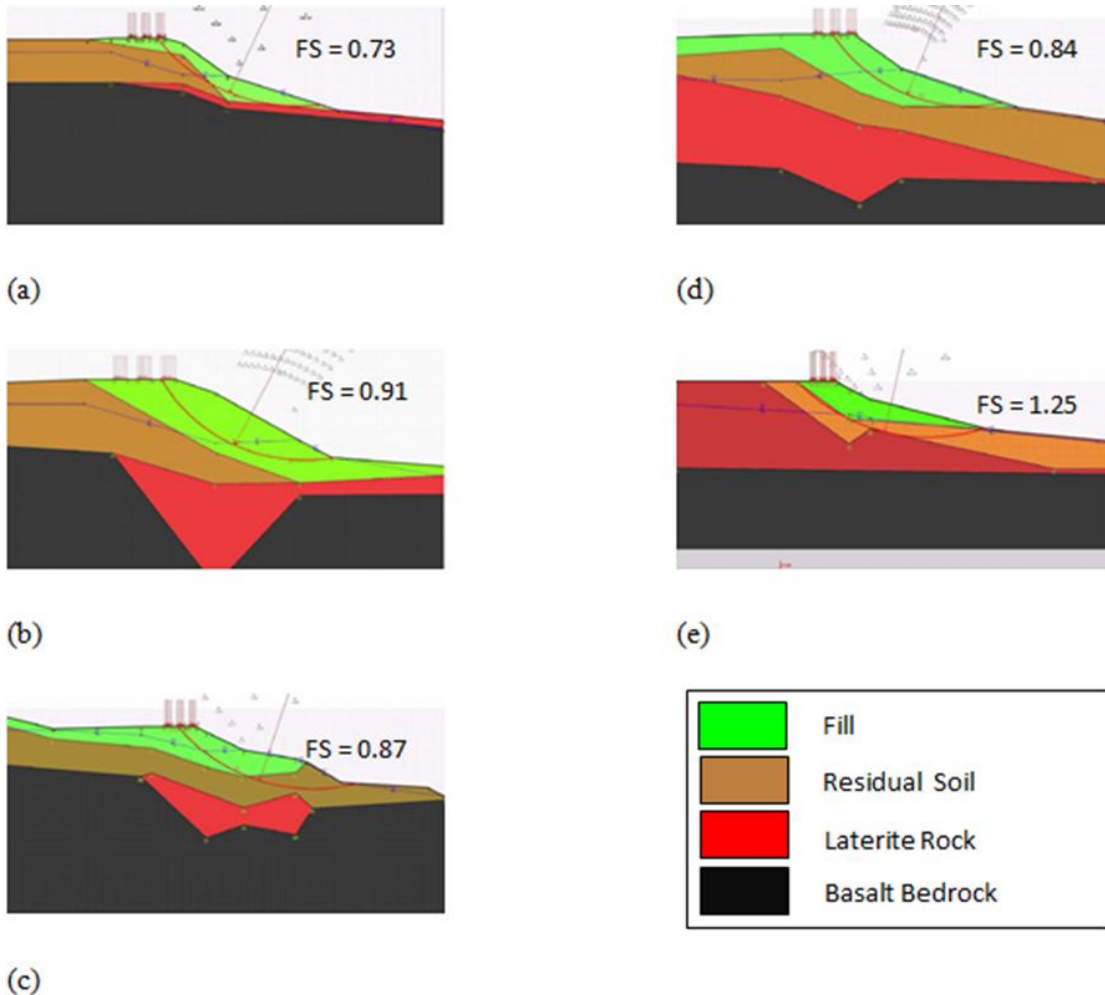
Table 6. Minimum safety factor during dry season with modified parameters

| Section | Safety factor |
|---------|---------------|
| A-A     | 1.01          |
| B-B     | 1.0           |
| D-D     | 1.03          |



Table 7. Modified geotechnical properties at selected sections

| Section | Strata Type | $c'$<br>kN/m <sup>2</sup> | $\phi'$ ° |
|---------|-------------|---------------------------|-----------|
| A-A     | Fill        | 10                        | 27        |
|         | Residual    | 20                        | 30        |
| B-B     | Fill        | 20                        | 27        |
|         | Residual    | 15                        | 29        |
| D-D     | Fill        | 20                        | 27        |
|         | Residual    | 15.2                      | 29        |



Figures 12a-e. Safety factor during wet season with modified parameters for section: (a) A-A; (b) B-B; (c) C-C; (d) D-D; and (e) E-E.



Intuitively, the difference in the numerical results and the field observations can be attributed to sampling disturbance and the inherent inhomogeneity of the samples collected during the site investigation. Unfortunately, much of these differences are difficult to quantify because of their stochastic nature. However, back analysis can be used to find the soil properties that result in a safety factor of unity for sections A-A, B-B and D-D. Table 6 shows the minimum safety factor recalculated in these sections using back calculated soil properties. The safety factors are now reasonably well predicted for all the sections. The effective shear strength parameters ( $c'$ ,  $\phi'$ ) of the fill and the residual soils from this back analysis are shown in Table 7. A quick comparison of Tables 7 and 4 shows that the parameters in sections A-A, B-B and D-D are now similar to those in sections C-C and E-E, thereby lending further confidence to the back-analyzed properties. For this reason, geotechnical properties from Table 7, and not Table 4, were adopted for sections A-A, B-B and D-D in the analysis that follows.

Figures 12a to 12e show the minimum safety factor and the location of critical circles in sections A-A to E-E for the wet (monsoon) season. In all the figures, the critical slip circle passes through the toe of the embankment, which is similar to the observations made at the site (see Figure 5). Similarly, the top of the circle in Figure 12c intersects the rail tracks and lie close to point X in Figure 2. The safety factor of all the 5 sections for the dry and the wet seasons are compared in Table 8. As can be seen, the safety factor reduced to less than one with the rise in ground water table in all sections, except in section EE. Figure 12e shows that only section E-E was stable during the wet season. This section was far beyond the failure zone shown in Figure 7. Regardless of the above observation, it is plausible that factors such as deep-rooted trees present at the site may have affected the safety factor. All the same, the effect of vegetation on the slope stability cannot readily be incorporated within this simplistic framework (Bernhardt et al. 2011).

*Table 8. Change in safety factor with the rise in ground water table*

| Section | Minimum safety factor |             |
|---------|-----------------------|-------------|
|         | Lowest GWT            | Highest GWT |
| A-A     | 1.01                  | 0.73        |
| B-B     | 1.0                   | 0.91        |
| C-C     | 1.37                  | 0.87        |
| D-D     | 1.03                  | 0.84        |
| E-E     | 1.43                  | 1.25        |

## SOIL STRENGTH

The above slope stability analysis only permits the estimation of the safety factor using the effective (or drained) shear strength parameters. It does not account for the change in strength of the soil due to the change in the degree of saturation as the rainwater percolates. An experimental programme was therefore designed to also study the effect of the change in the degree of saturation on the strength of the residual soils. A series of routine UU-triaxial shear tests were conducted on remoulded and reconstituted samples at 100 to 200 kN/m<sup>2</sup> cell pressure. The samples were compacted at constant void ratios but different degree of saturation. The dry unit weight of all the samples was within the range of 13.5 to 14 kN/m<sup>3</sup>. The tests were carefully conducted to avoid any change in water content during the testing procedure. However, it must be noted that since most of the samples were partially saturated, the tests were not truly undrained. There was no arrangement to measure the pore pressure suction because its effect was considered to be insignificant in view of the short duration of the test (Vanapalli et al. 1999). Figure 13 shows the variation of the undrained shear strength,  $s_u$  with the degree of saturation,  $S$ . Despite the scatter of the data points, the results appear to suggest that the water content has significant influence on the strength of residual soils. For instance, the figure shows that an increase in  $S$  from 0.1 to 1 caused  $s_u$  to decrease by over 100%. Notwithstanding the above, the results also permit a semi-empirical relationship to be fitted to the data:

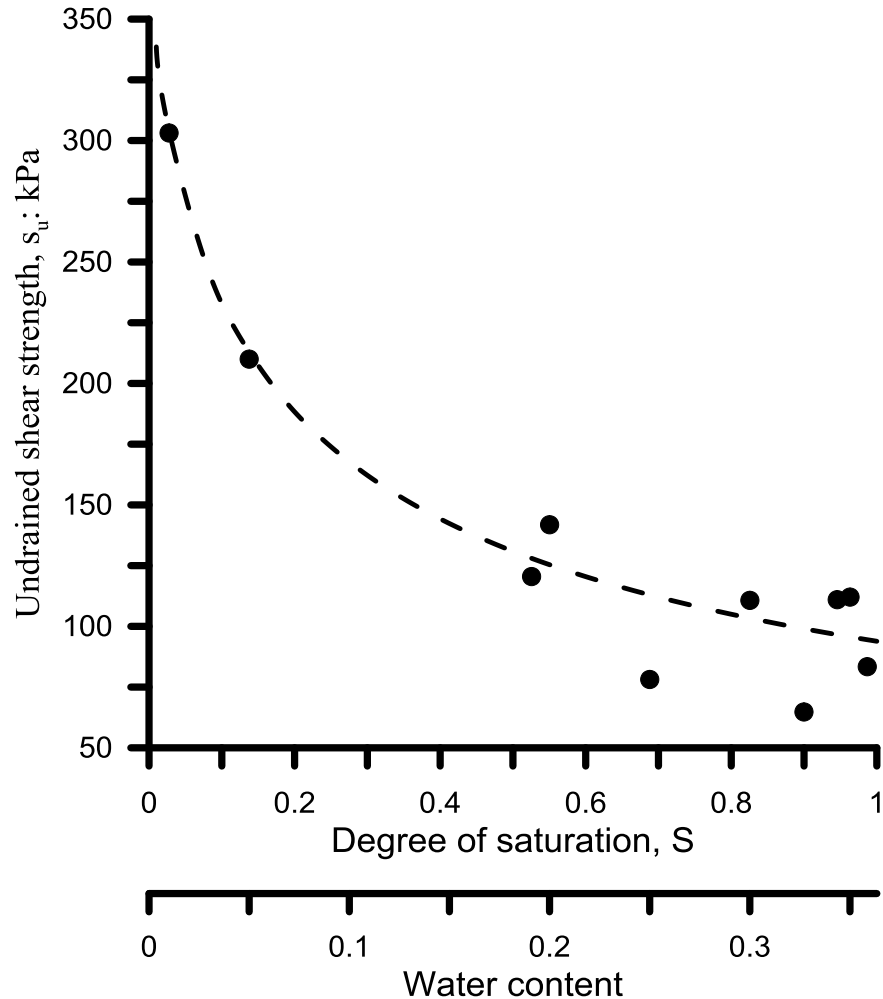
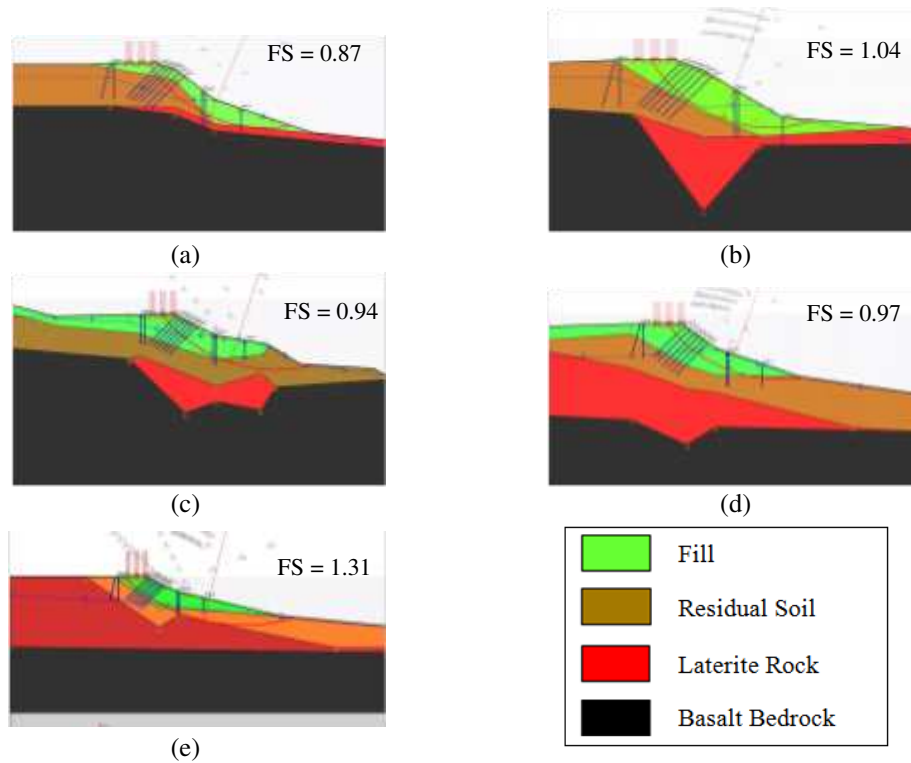


Figure 13. Variation of undrained shear strength, with degree of saturation at constant void ratio/dry density.

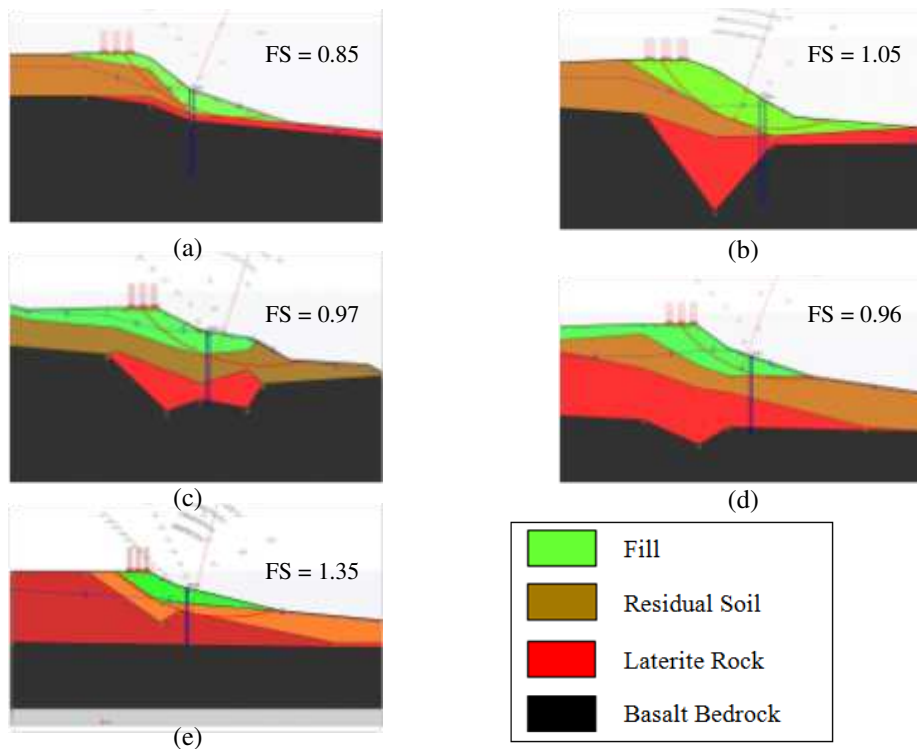
$$s_u = \left[ \frac{385}{1 + (5.3S)^{0.68}} \right] \quad (1)$$

### REINFORCED SLOPE FAILURES IN 2006 AND 2008

Soil nails and micropiles were installed in November 2005. These reinforcements failed and could not arrest the slope movement during the 2006 monsoon. Subsequently, two new rows of micropiles installed in January 2007 also failed during the 2008 monsoon. It was therefore appropriate to also study the stability of the 2006 and 2008 reinforced slope failures. In this analysis, the location, diameter and spacing of the reinforcement elements were taken from Table 1. Ground conditions and the slope geometry were identical to those used in the previous case. Figures 14a-e and 15a-e show the minimum safety factors and the location of critical circles in sections A-A to E-E for the 2006 and 2008 wet (monsoon) season, respectively. As can be seen, the safety factor is less than one in sections A-A, C-C and D-D for both years, indicating that the soil nails and micropiles installed in November 2005 and January 2007 were indeed inadequate to resist the slope movement. It is also interesting to note from Figures 12a-e and 14a-e to 15a-e that the reinforcement has little influence on the shape and size of the critical slip circle.



Figures 14a-e. Safety factor and critical slip circle during wet season with November 2005 ground improvement scheme for section: (a) A-A; (b) B-B; (c) C-C; (d) D-D; and (e) E-E.



Figures 15a-e. Safety factor and critical slip circle during wet season with January 2007 ground improvement scheme for section: (a) A-A; (b) B-B; (c) C-C; (d) D-D; and (e) E-E.

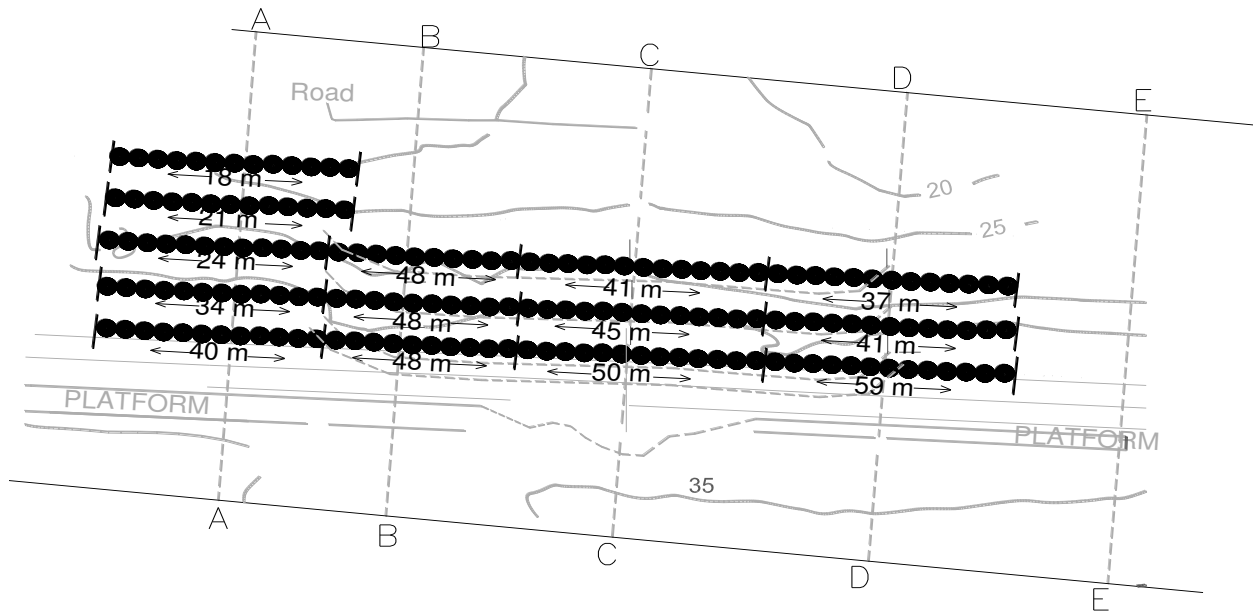
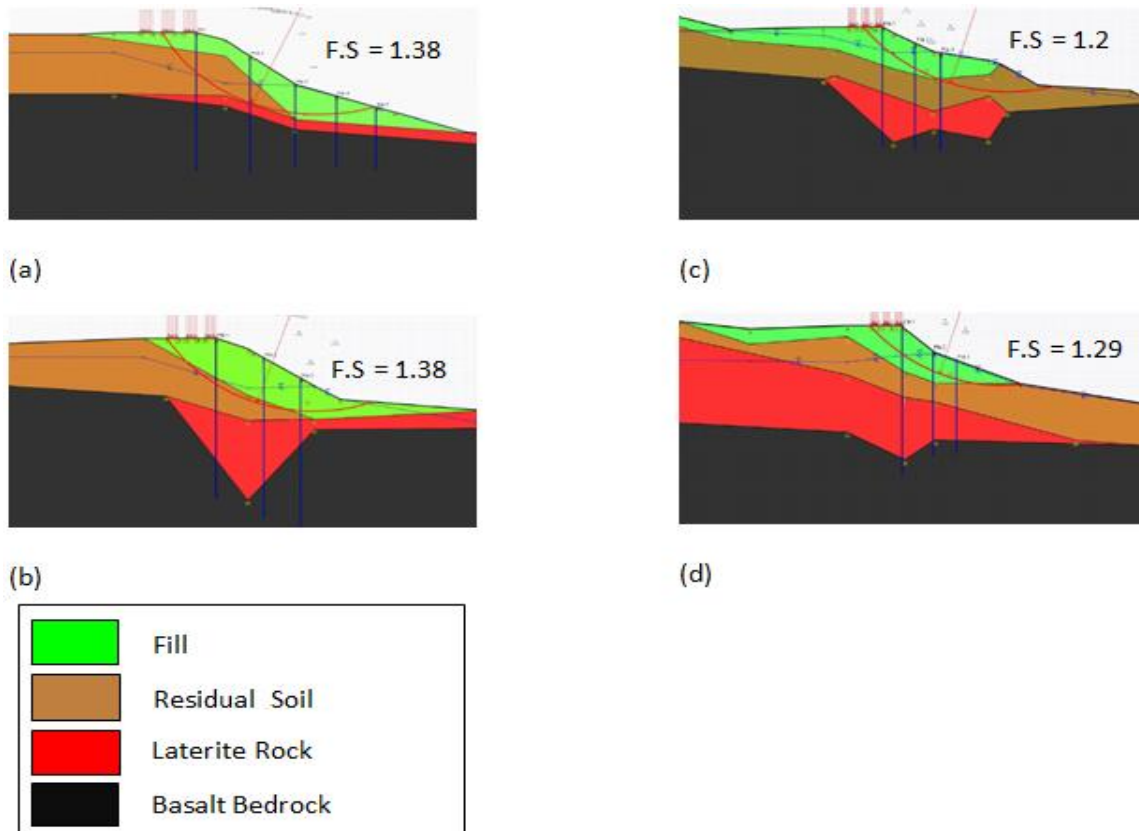


Figure 16. Schematic layout of the proposed 1.2m diameter bored pile wall at 1.2m c/c (contiguous bored pile wall). Note: Numbers below the piles indicate length of the piles.



Figures 17a-d. Safety factor during wet season with proposed contiguous bored pile for section: (a) A-A; (b) B-B; (c) C-C; and (d) D-D.



*Table 9. Location and length of pile in contiguous bored pile wall*

| Section | Pile row | Distance from edge of the platform, m | Pile length, m |
|---------|----------|---------------------------------------|----------------|
| A-A     | 1        | 20                                    | 40             |
|         | 2        | 33                                    | 34             |
|         | 3        | 43                                    | 24             |
|         | 4        | 53                                    | 21             |
|         | 5        | 63                                    | 18             |
| B-B     | 1        | 20                                    | 48             |
|         | 2        | 33                                    | 48             |
|         | 3        | 43                                    | 48             |
| C-C     | 1        | 23                                    | 50             |
|         | 2        | 36                                    | 45             |
|         | 3        | 46                                    | 41             |
| D-D     | 1        | 24                                    | 59             |
|         | 2        | 37                                    | 41             |
|         | 3        | 47                                    | 37             |

Note: All piles are 1.2m in diameter

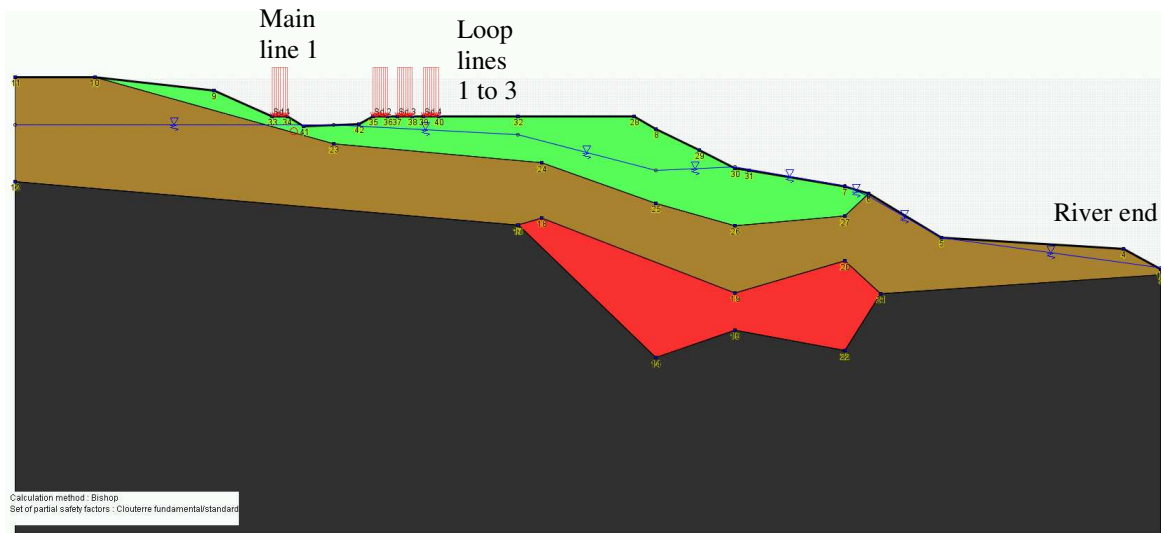


*Figure 18. Section C-C with new rail alignment. The main alignment consists of 3 loop lines and 1 main line.*



## STABILITY OF SLOPE REINFORCED WITH PILES

One possible solution to enhance the stability of the slope was with the use of large diameter piles to retain the (failed) soil mass. In this case, safety factors of sections A-A to E-E were also deduced by assuming that the slope was reinforced with single or multiple rows of contiguous bored pile wall constructed parallel to the platform. Figure 16 shows the schematic layout of the proposed bored pile wall. The 1.2m diameter piles terminated below the slightly-to-moderately weathered basalt rock because of which sections B-B and C-C had long piles to provide adequate anchorage (Table 3). Table 9 shows the location and length of the piles used in the analysis. Figures 17a-d show the minimum safety factor and the location of critical circles in sections A-A to D-D for the wet season when the slope is reinforced with contiguous bored pile wall. As can be seen, the minimum safety factor increased up to 1.2 and 1.38 with the use of contiguous bored pile wall.

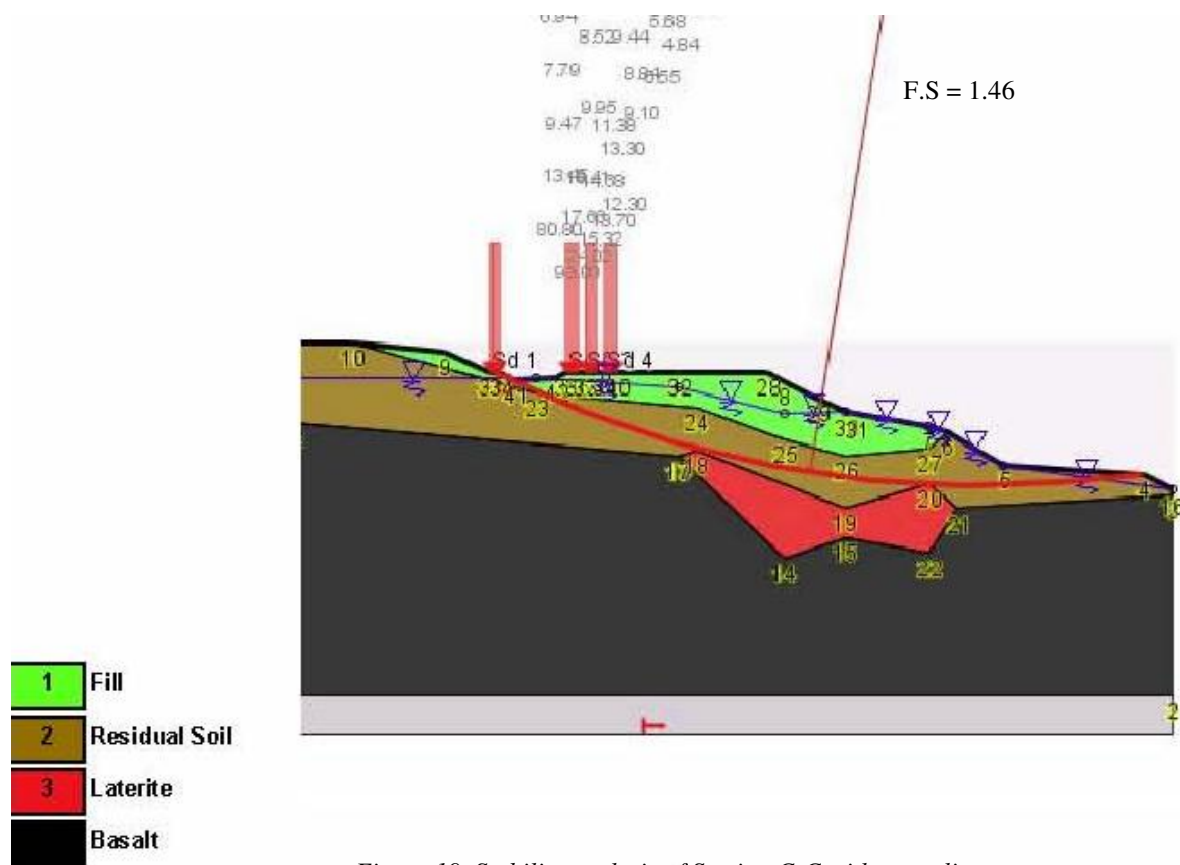


Figure 19. Stability analysis of Section C-C with new alignment.

## STABILITY OF THE SLOPE WITHOUT REINFORCEMENT AND WITH NEW RAIL ALIGNMENT

The cost to use the bored pile wall was over 200 million Indian Rupees (US\$ 3.6 million) and appeared to be prohibitive. As an alternative to this design, the old rail alignment was removed and replaced by a new alignment. The new alignment consisted of 3 loop-lines and 1 main-line. Figure 18 shows section C-C along with the location of the new alignment. In this section, the top left side of the hill was slightly levelled to accommodate the main line and the loop lines. Section C-C was chosen because the new alignment was closest to the failure surface at this section. The horizontal distance from the vertex of the failure surface and the 4 lines was 16m, 21.3m, 26.2m and 46.4m, respectively. The stability of the slope was then reinvestigated using the computer program Talren-4 (Terrasol 2005). As in the previous case, all the lines were loaded by 125 kN/m<sup>2</sup>. This assumption was unduly conservative in absence of strict guidelines (RDSO 2003b). Nonetheless, it permitted trains with more overtaking opportunities on the passing-loops. The ground water level was modeled using the highest RL recorded in Table 5. The failure circles are shown in Figure 19. As can be seen, the minimum safety factor is



---

more than 1.4. The slope was therefore considered to be safe and unlikely to fail under the new loads. This new alignment has been implemented since 2011. It has been constructed at less than 20 percent of the cost incurred to improve the ground. The railways have also removed the speed restriction at Nivsar which has resulted in additional savings during the monsoon.

## CONCLUSION

This paper presented data on the slope stability of an embankment in residual soils and its performance. Shear strengths from back-analysis of the unstable slopes provided safety factors that were reasonable for all sections in dry as well as wet season. Water content significantly affects the shear strength of residual soils. The results appear to suggest that the undrained shear strength is reduced by over 100% when the soils become saturated from the dry state. These results also imply that a slope which is marginally stable during the dry-season is likely to fail during the monsoon, unless its height is reduced by about one-half.

Soil nails and micropiles installed in 2005 and micropiles installed in 2007 failed to arrest the slope movement during the monsoons. In other words, RDSO's (2003b) guidelines on earthwork should be improved to account for the train loads and to minimize serious design errors.

## ACKNOWLEDGEMENT

This work was supported by the Industrial Research and Consultancy Centre at IIT Bombay under project code 10CE084. The field drilling, sampling and testing was conducted by DBM Geotechnics, Mumbai. The second author would also like to acknowledge the financial support from IITB in the form of research scholarships which enabled her to contribute to this study.

## REFERENCES

- Bernhardt, M., Briaud, L. J., Kim, D., Leclair, M., Storesund, R., Lim, G. S., Bea, G. R. and Rogers, D. J. (2011). "Mississippi river levee failures: June 2008 flood". *International Journal of Geotechnical Engineering Case Histories*, 2(3), 127-162.
- Chen, W. and Hill, C. (2005). "Evaluation procedure for coordinate transformation". *Journal of Surveying Engineering*, 131(2), 43-49.
- RDSO (2003a). "Code of practice for the design of sub-structures and foundations of bridges". Geotechnical Engineering Directorate, Research Designs and Standards Organisation, Government of India, Ministry of Railway, 51pp.
- RDSO (2003b). "Guidelines for earthwork in railway projects". GE:G-1, Geotechnical Engineering Directorate, Research Designs and Standards Organisation, Government of India, Ministry of Railway, 89pp.
- RDSO (2005). "Guidelines for cuttings in railway formations". GE:G-2, Geotechnical Engineering Directorate, Research Designs and Standards Organisation, Government of India, Ministry of Railway, 183pp.
- Singh, P. (2010). "Engineering and general geology". S.K. Kataria & Sons, New Delhi, 600pp.
- Spencer, E. (1967). "A method of analysis of the stability of embankments assuming parallel inter-slice forces". *Geotechnique*, 17(1), 11-26.
- Taylor, D.W. (1948). "Fundamental of soil mechanics". John Wiley & Sons, New York.
- Terrasol, (2005), Talren 4: Stability analysis for geotechnical structures with or without reinforcements". Montreuil Cedex, France (2005). <http://www.terrasol.com>
- Vanapalli, S.K., Fredlund, D.G., Pufahl, D.E., (1999). "The influence of soil structure and stress history on the soil-water characteristics of a compacted till". *Geotechnique*, 49(2), 143-15.



INTERNATIONAL JOURNAL OF  
**GEOENGINEERING  
CASE HISTORIES**

*The Journal's Open Access Mission is  
generously supported by the following Organizations:*



Access the content of the *ISSMGE International Journal of Geoengineering Case Histories* at:  
[www.geocasehistoriesjournal.org](http://www.geocasehistoriesjournal.org)